Int. J. Aquat. Biol. (2024) 12(4): 330-339
ISSN: 2322-5270; P-ISSN: 2383-0956
Journal homepage: www.ij-aquaticbiology.com

Original Article

Preparation and characterization of nano-antioxidant via ionically cross-linked silymarin nanoparticles with chitosan polymer as a carrier

Nisreen Yasir Jasim*[1], Rashad Fadhil Ghadhban

Department of Physiology, Pharmacology and Biochemistry, College of Veterinary Medicine, University of Basrah, Basrah, Iraq.

Abstract: This study investigates the preparation and characterization of nano-antioxidant formulations using ionic cross-linking between silymarin and chitosan polymer to produce Silymarin-Chitosan Nanoparticles (S-CsNPs). Silymarin, *Silybum marianum*, is renowned for its hepatoprotective properties, attributed to its antioxidant activity. However, its clinical efficacy is limited by poor oral bioavailability, primarily due to low water solubility and rapid systemic clearance. To address these challenges, this research uses nanotechnology to enhance silymarin's solubility, stability, and bioavailability. Through ionic gelation methods, silymarin is encapsulated within chitosan, a biocompatible and biodegradable polymer, to protect it from physicochemical degradation and enhance therapeutic efficacy. Initial findings highlight the potential of this nanoparticulate system in improving dissolution. Based on the results, silymarin was effectively loaded onto chitosan. SEM analysis showed that the size of the nano-silymarin particles ranged from 25.81 to 43.03 nm. Additionally, XRD analysis confirmed the crystalline nature of the S-CsNPs. The study also observed a relatively smooth surface and homogeneous distribution of the S-CsNPs particles.

Article history:
Received 21 July 2024
Accepted 22 September 2024
Available online 25 August 2024

Keywords:
Nano Silymarin
Antioxidant
Ionic Gelation
S-CsNPs

Introduction

Silymarin is a complex derived from the seeds of milk thistle (*Silybum marianum* (L.) Gaertn), known for its hepatoprotective properties (Woo et al., 2007). It comprises seven flavonoids: silybin A, silybin B, isosilybin A, isosilybin B, silydianin, silychristin, and taxifolin. Silymarin protects the liver from toxins, including heavy metals, pesticides, alcohol, acetaminophen, and CCl4 (Macit et al., 2023). Moreover, it is a potent antioxidant (Camini and Costa, 2020). Silymarin exhibits low oral bioavailability due to its poor water solubility. Nanotechnology offers a promising approach by improving solubility, stability, and bioavailability to enhance its dissolution rate. The low bioavailability of silymarin may be due to its poor water solubility in gastric pH, inadequate permeability across gut epithelial cells, and rapid elimination. Encapsulating drugs within polymeric nanoparticles is currently employed to develop new, more effective therapies. The use of biocompatible and biodegradable polymers offers several advantages for these formulations. These include protecting active ingredients against environmental and physiological factors, reducing the number of doses to minimize drug-related adverse effects, and improving bioavailability. Various methods and materials are now used to synthesize nanoparticles for biomedical applications, from carbon-derived structures to metallic and lipid particles. Among polymer-based methods, ionotropic gelation stands out due to its affordability and ease of execution in daily laboratory procedures (Pedroso-Santana and Fleitas-Salazar, 2020). Therefore, this study investigates the preparation and characterization of nano-antioxidant formulations using ionic cross-linking between silymarin and chitosan polymer to produce Silymarin-Chitosan Nanoparticles (S-CsNPs).

Materials and Methods

Biosynthesis of S-CSNPs: Chitosan (Sigma-Aldrich, Germany) and 5% Silymarin (Xi'an Natural Field Bio-

*Correspondence: Nisreen Yasir Jasim
E-mail: pgs.nisreen.yasir@uobasrah.edu.iq

DOI: https://doi.org/10.22034/ijab.v12i4.2316

Technique Co., Ltd, China) were combined in equimolar ratios, and the condensation process was done in the presence of xylene using the Dean-Stark (Clevenger, OEM, India) apparatus until the theoretical quantity of water was separated. Chitosan amide product was separated by filtration, washed several times with methanol, hot distilled water, and ethanol, and then dried in an electric oven at 50℃ and weighed (El-Ghaffar and Hashem, 2010). S-CSNPs were obtained by use of an ionic-gelation method by adding Tripolyphosphate (TPP) with CS-Silymarin adduct as follows: Dissolve 5 mg/ml CS-Silymarin in an acetic acid solution (1% w/v) until the solution becomes clear. Then, TPP was added to the CS-Silymarin solution in ratios of 1: 2.5 (w/w %) while continuously stirring at room temperature for 6 hours. The nanoparticles were separated and washed several times, and the supernatant layer was removed before the precipitate was resuspended in water and dried (Nasti et al., 2009).

Characterization of S-CSNPs: Several methods were used to characterize (morphological, structural, and size) S-CsNPs. These characterization tests were done in the material research laboratories at the Ministry of Sciences and Technology Environment and Water Research and Technology Director (EWRTD) Iraq. The absorbance spectra of the Silymarin-CsNPs solution were measured by UV-VIS spectrophotometer. All spectra were taken in a quartz cell with a 1 cm optical path at room temperature. Deionized distilled water was utilized as a control. The absorption was calculated using 200-800 nm. The concentrated samples were diluted at 1:10 (Agarwal et al., 2018). The characterization of functional groups on the surface of chitosan and chitosan-plant extract (Silymarin-CSNPs) was investigated by FTIR analysis (Shimadzu, Japan), and the spectra were scanned at a resolution of 4 cm^{-1} in the range of 400-4000 cm^{-1}. By spreading the samples on a microscope slide, the samples were produced according to standard methods (Agarwal et al., 2018). Each sample was prepared as a pellet in potassium bromide (KBr) at a 1:99 ratio of sample to KBr for FTIR; after that, the sample was examined (Oh et al., 2019).

A scanning electron microscope (SEM) was employed to analyze the morphology of the formed nanoparticles. The samples were morphologically characterized using a Brucker SEM. By spreading the materials on a glass slide, the samples were prepared according to standard methods (almost seven drops on the slide). After that, the sample was put through its tests. According to Atangana et al. (2019). A small drop of Silymarin nanoparticles was placed on a carbon-coated copper grid and allowed to dry using the mercury lamp for 5 min. Then, readings were taken at a magnification of 5000, 10000, 20000, and 50000x with steady voltage (Dimitrijevic et al., 2013). The surface morphology of the nanoparticles was visualized in Atomic Force Microscope Contact mode under normal atmospheric conditions. Samples of nanoparticle solution drops on a glass slide (1×2 cm). The samples dried, the slide was dispersed on the AFM sample stage, and analysis was carried out according to the standard procedure (Du et al., 2008).

The X-ray diffraction (XDR)technique was applied to probe the structure of S-CsNPs and crystalline nature at 2θ angle by Cu-Kα radiation operated at 40 kV and 30 mA. The crystallite size of S-CsNPs was calculated using the Debye Scherrer equation as $D = K\lambda\ \beta\ cos\ \theta$, where D = diameter of NPs dimension, K = a constant value (0.94 is used along with cubic symmetry to harmonize spherical crystallites), λ is the X-ray wavelength, β = Full Width at Half Maximum (FWHM) and θ (Bragg angle) = angle of diffraction (Sarvamangala et al., 2013).

Results and

S-CsNPs synthesis and characterization: The nanoparticles were created by interactions between the positively charged Chitosan and the negatively charged phosphate groups of TPP in the ionic gelation technique. When chitosan reacts with TPP, the amine groups of the chitosan can cross-link with the phosphine groups of TPP to create nanoparticles. During the action, the chitosan's molecular structure will be altered, resulting in a change in solubility in an acid solution and a gel-like solution or a liquid form (Kahdestani et al., 2021). The appearance of a clear

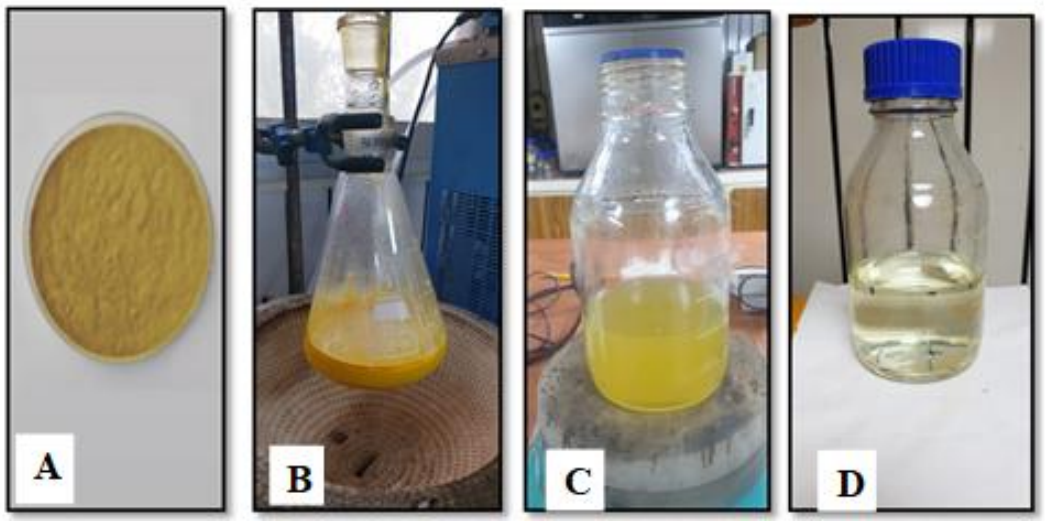

Figure 1. Steps of the S-CSNPs preparation. A: Dried standard, B: Reflux stage of silymarin with chitosan and precipitate formation on the wall, C: Silymarin /CS adduct, and D: S-CSNPs.

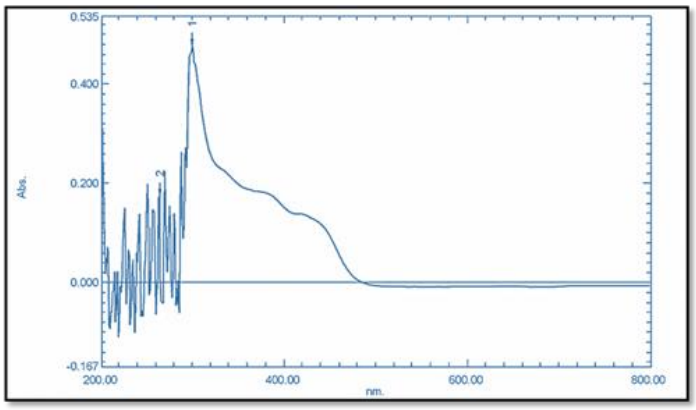

Figure 2. UV-visible spectral analysis of standard Silymarin.

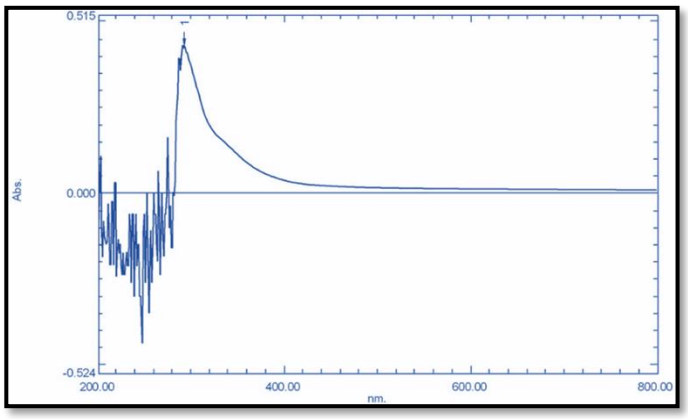

Figure 3. UV-visible spectral analysis of S-CSNPs.

color indicates the formation of nanoparticles loaded with the standard plant extract (standard silymarin) (Fig. 1).

UV–visible spectroscopy is a primary step in confirming the synthesis of S-CSNPs. The absorbance of standard Silymarin extract and nanosilymarin (S-CSNPs) were measured by scanning the ready solution with UV-visible spectrophotometer wavelengths (200- 800 nm) at room temperature for standard Silymarin extract (Fig. 2) and for nanosilymarin (S-CSNPs) (Fig. 3). There are two different peaks of optical absorbance values of standard Silymarin the highest absorbance value was 0.477 at wavelength 299 nm, and the lowest absorbance value was 0.175 at wavelength 263 nm. The absorbance at wavelengths was calculated as shown in standard Silymarin (Table 1). The absorbance value was 0.428 at wavelength 292 nm for S-CSNPs (Table 2).

Fourier transformation infrared spectroscopy (FTIR): FTIR analysis was conducted to analysis the chemical composition of the nano solution prepared by loading silymarin onto chitosan (S-CSNPs.) The obtained spectrum revealed distinct peaks, indicating the infrared absorption by the compounds present in the solution. Analyze these peaks to identify the chemical interactions between chitosan and silymarin in the S-CSNPs solution because the Fourier transform infrared spectra are useful for observing functional groups, elucidating their role in the formation and stability of the nanostructure. FTIR analysis was employed to identify functional groups responsible for reducing Chitosan CS to S-CSNPs and their stabilization.

Table 1. UV-visible spectral analysis result of standard Silymarin.

Peak No.	Wavelength	Absorbance
1	299.00	0.477
2	263.00	0.175

Table 2. UV-visible spectral analysis result of S-CSNPs.

Peak No.	Wavelength	Absorbance
1	292.00	0.428

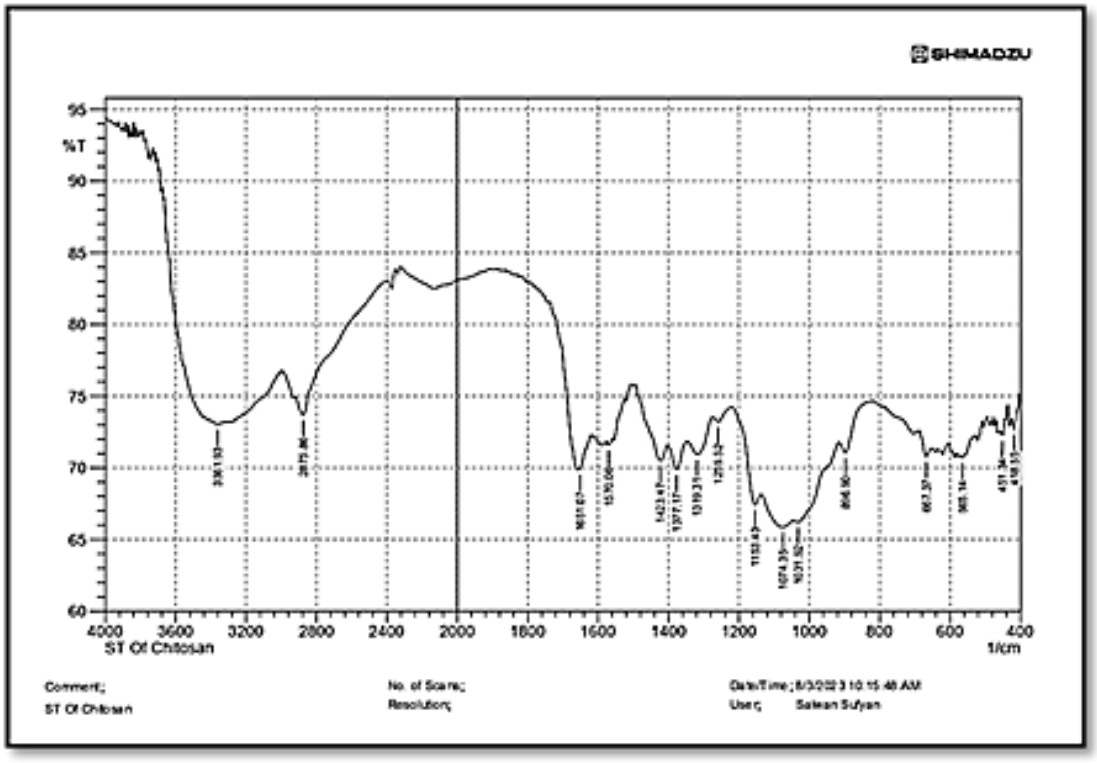

Figure 4. FTIR Spectra Pattern of CS.

The interpretations of the peaks observed in the FTIR analysis of chitosan (Fig. 4). The peak at approximately 3361.93 cm^{-1} indicates the presence of hydroxyl (-OH) and amino (-NH) groups, characteristic of the natural polymer chitosan. Therefore, the functional group for this peak can be assigned as amino and hydroxyl groups. The peak at around 2875.86 cm^{-1} indicates the presence of carbon-hydrogen (stretching-CH alkane group) bonds, which are also part of the structure of chitosan. Therefore, the functional group for this peak can be assigned as carbon bonds. The peak at approximately 1651.07 cm^{-1} indicates the presence of the amide group (stretching C=O Carbonyl bond), suggesting the presence of amides in chitosan. Therefore, the functional group for this peak can be assigned as amides. The peak at 1570.06 cm^{-1} indicates secondary vibrations of amides and C=N stretching in chitosan. Then, the functional group for this peak can also be assigned as amides. Chitosan consists of glucosamine units linked by β-(1,4) glycosidic bonds, which may contain C=N bonds in the molecular structure. The mentioned peak suggests the presence of these bonds in chitosan. Hence, the functional groups identified based on the interpretation of the peaks include amino and hydroxyl groups, Carbon bond, and amides.

Figure 5 shows FTIR analysis of S-CsNPs 3757.33 and 3433.29 cm^{-1} that are attributed to the stretching vibrations of hydroxyl groups (O–H stretching, Phenols/Alcohols), which are a common functional

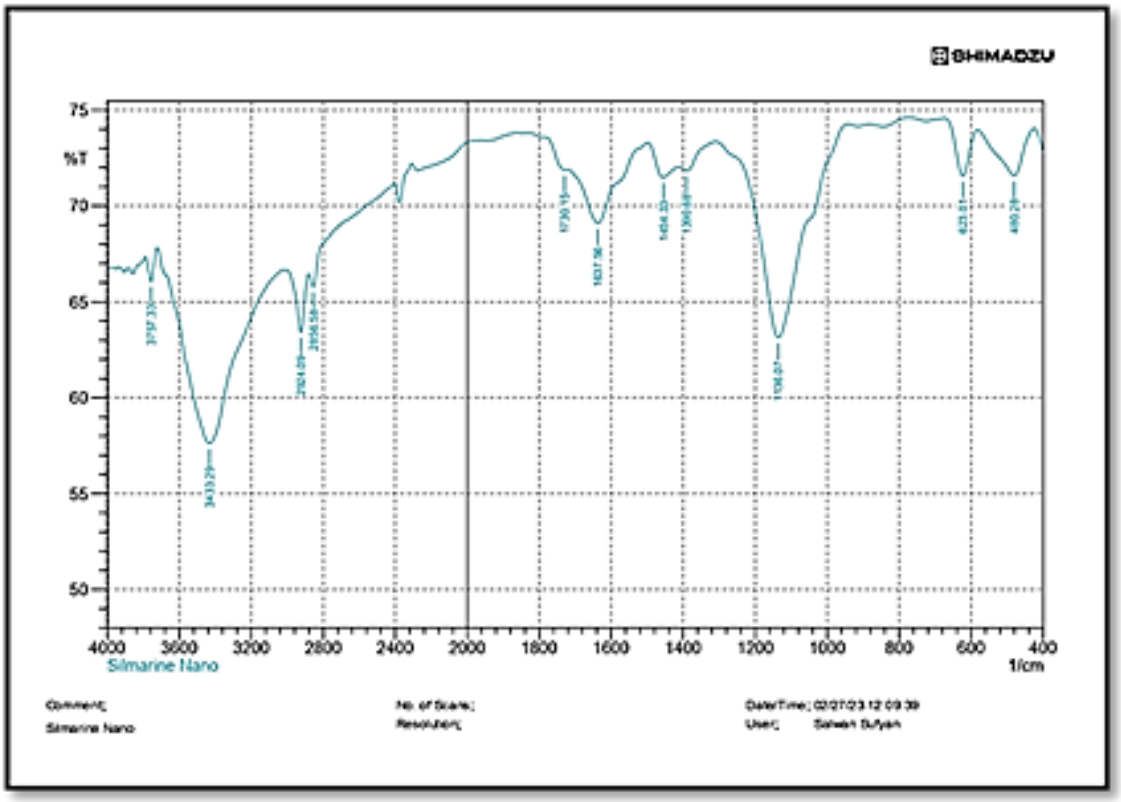

Figure 5. FTIR Spectra Pattern of S-CSNPs.

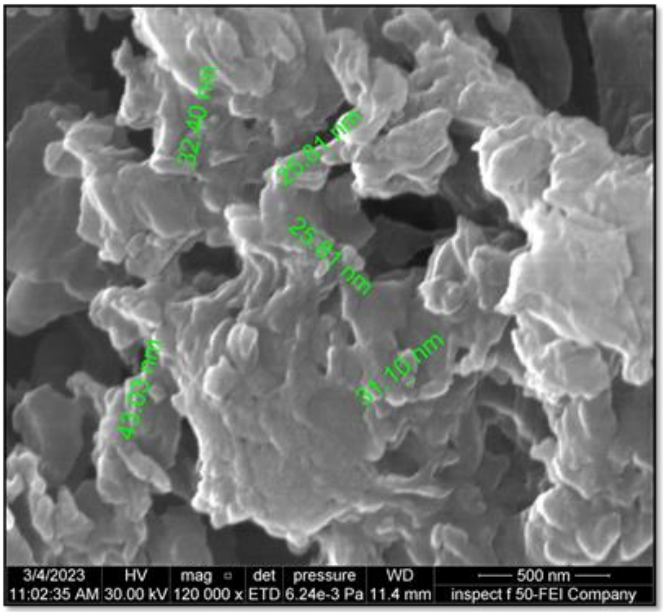

Figure 6. Scanning Electron Microscopy (SEM) image of S-CSNPs.

group in silymarin and chitosan. 2924.09 and 2856.58 cm^{-1} are associated with the stretching vibrations of carbon-hydrogen bonds (C–H stretching, Alkanes), which may appear as a result of chitosan, while 1730.15 cm^{-1} is typically attributed to the stretching vibrations of carbonyl groups (C=O stretching, Esters), which associated with silymarin molecules. 1637.56 cm^{-1} peak is likely associated with the stretching vibrations of the amide (C=O stretching) groups, which are common functional groups in chitosan and silymarin. 1454.33 and 1390.68 cm^{-1} are bending C-H alkanes group. 1136.07 cm^{-1} is related to the stretching vibrations of carbon-oxygen bonds (C-O alcohol) and 623.01 cm^{-1} to C-H aromatics group. This demonstrates that chitosan functional groups interact with Silymarin NPs loaded via ionic gelation.

Scanning Electron Microscope: The morphology and size of S-CSNPs were investigated using an SEM (Fig. 6). S-CSNPs have a spherical appearance, a diameter range of 25.81-43.03 nm, and a relatively homogeneous morphology.

Atomic force microscopy (AFM): AFM provides precise, three-dimensional surface topography and nanostructure analysis with high accuracy at the nanometer scale. This instrument enables researchers to gain deeper insights into surface properties and interactions, contributing to the development of new applications in areas such as nanotechnology, materials science, and surface chemistry. The

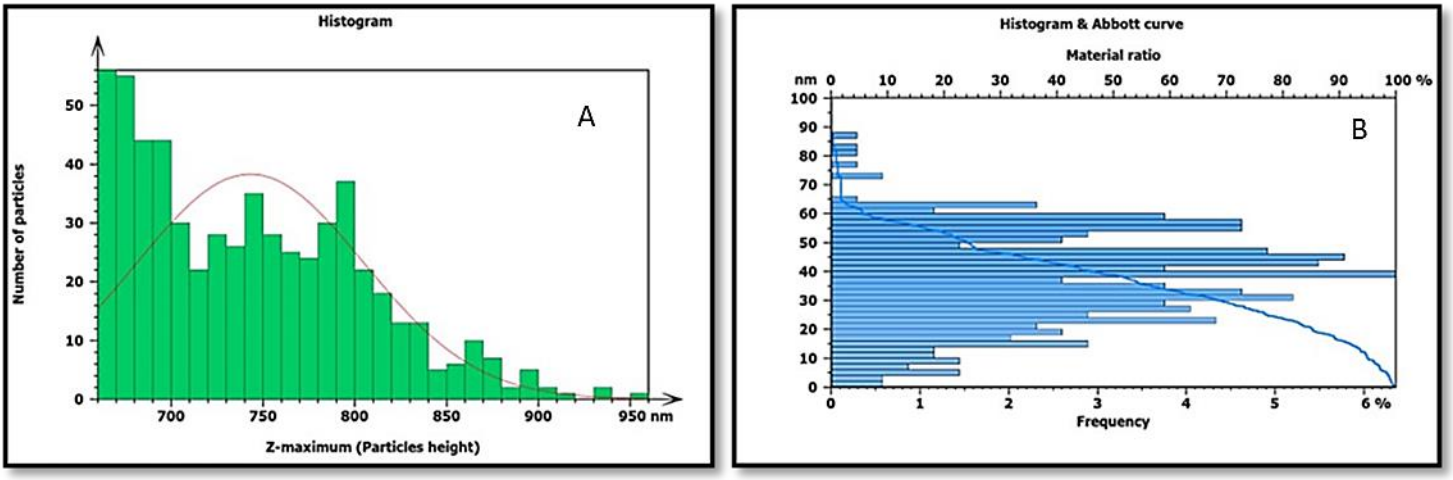

Figure 7. Distribution of S-CSNPs according to particles size (A) Histogram Z -maximum (B) Abbott curve

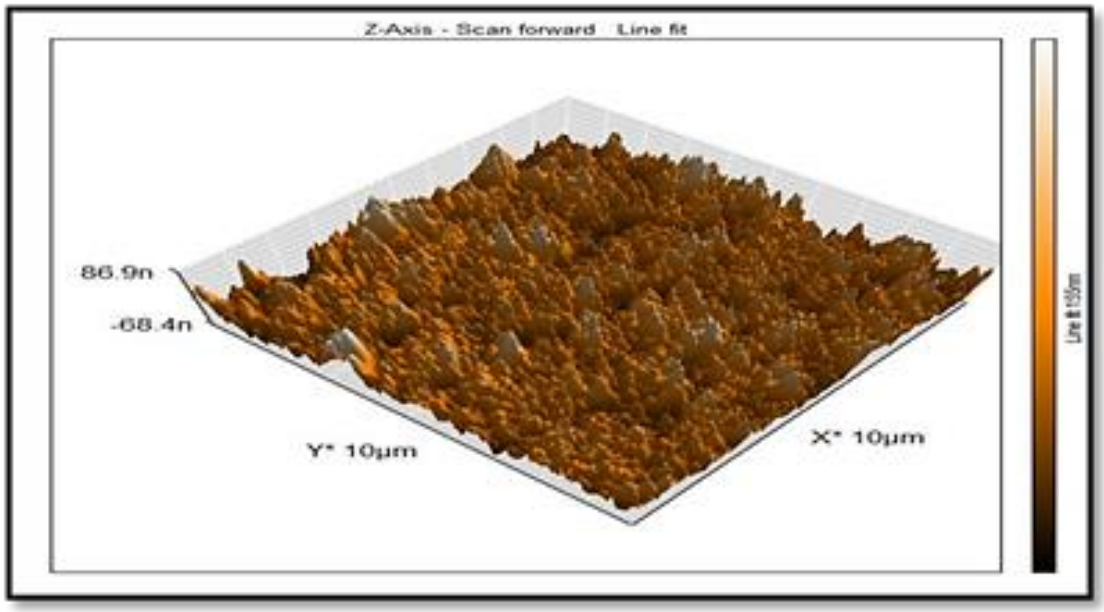

Figure 8. An AFM-showed three-dimensional image of S-CSNPs revealed a population of homogeneous particles with a regular surface shape.

effectiveness of the AFM relies on atomic force technology, where a nanoscale tip is used to measure changes in interactive forces between the tip and the sample being studied. Atomic Force Microscopy images were used to measure the topography of the surface and particle size of S-CSNPs; the largest size has high frequencies ranging from 40 to 50 nm, extending from 0 to 80, and the mean height of 11.40 nm (Figs. 7, 8).

X-ray diffraction: The XRD technique determines the crystalline structure of S-CSNPs by directing X-rays onto a sample and recording the reflections resulting from the interaction of the X-rays with the atoms in the sample. The XRD pattern of chitosan exhibited two characteristic broad diffraction peaks at 2θ around 9.63 and 20.53, which are typical fingerprints of semi-crystalline chitosan (Fig. 9). Figure 10 shows the distinct S-CSNPs peaks, which shows its main peaks of 2θ value at 18.71◦, 22.68◦, 23.61◦,25.62◦,31.92◦,33.98◦, 40.19◦, 42.30◦, 45.49◦, 46.24◦, 48.22◦, 52.51◦, 56.72◦, 58.14◦, 64.08◦ and 66.74 ◦.

Discussions

Biosynthesis of S-CSNPs: Encapsulating drugs within polymeric nanoparticles or microparticles are currently being employed to search for new, more effective therapies. Utilizing biocompatible and

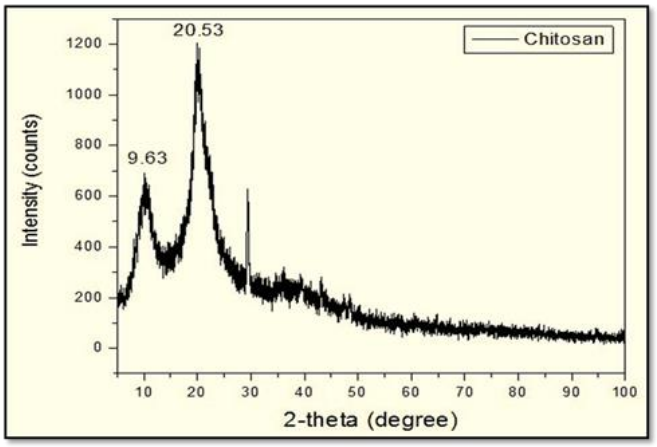

Figure 9. Diffractogram of CS (Chandra Dey et al., 2016).

biodegradable polymers offer several advantages, including protecting active ingredients from environmental and physiological agents, reducing the number of required doses, thereby decreasing drug-related side effects, and enhancing bioavailability. Ionotropic gelation (IG) is a technique that enables the creation of nanoparticles and microparticles through electrostatic interactions between two ionic species under specific conditions. One of these species must be a polymer. When a drug or bioactive molecule is introduced into the reaction, it can trap between the polymer chains, encapsulating within the nanoparticle or microparticle structure. This formulation allows for controlled drug release and offers additional benefits, such as co-encapsulation of multiple molecules, targeted particle functionalization, and extended bioactivity duration of the drug (Pedroso-Santana and Fleitas-Salazar, 2020).

In this work, Silymarin nanoparticles were prepared using the ionotropic gelation method, loading onto the polymer chitosan. Chitosan nanoparticles may be synthesized via the gelation method, which is based on cross-linking of anionic molecules (TPP) (Muzzarelli, 2009; Voron'ko et al., 2016). The cationic behavior of chitosan (CS) in the presence of diluted acids and the polyanionic character of sodium tripolyphosphate (TPP) are advantageous. Positively charged CS amino groups crosslink with negatively charged phosphate groups to form hydrogels. Chitosan nanoparticles loaded with silymarin were prepared, and then the TPP was added

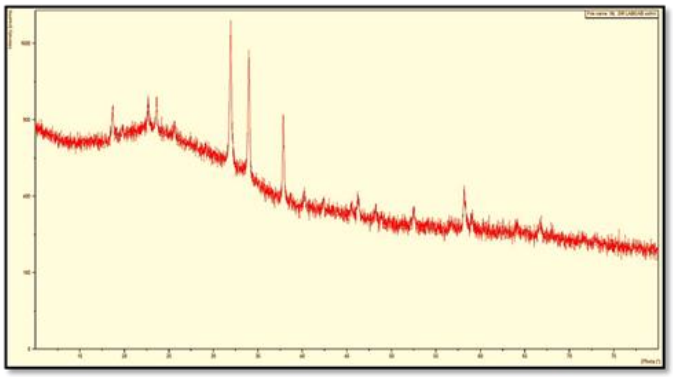

Figure 10. Diffractogram of S-CSNPs.

to form nano silymarin (S-CSNPs). When chitosan reacts with TPP, the amine groups of the chitosan can cross-link with the phosphine groups of TPP to create nanoparticles. During the action, the chitosan's molecular structure will be altered, resulting in a change in solubility in an acid solution and a gel-like solution or a liquid form (Kahdestani et al., 2021).

Characterization of synthesized S-CSNPs: UV spectroscopy analysis showed two peaks for the original silymarin extract at 299.00 nm (absorbance 0.477) and 263.00 nm (absorbance 0.175). S-CsNPs exhibited a single peak at 292.00 nm (absorbance 0.428. The decrease in the absorbance value at the wavelength 292.00 nm from 0.477 in the standard silymarin extract to 0.428 nm in S-CSNPs and the disappearance of the wavelength 263.00 nm in the Silymarin in the original extract indicates the formation of the nanomaterial and the successful loading of the silymarin extract on chitosan nanoparticles. This result suggests that the nanoparticle formation process has altered the UV spectral properties of silymarin, likely due to interactions with chitosan, changes in molecular distribution, structural modifications, or stability effects, and this result agreed with the findings of Chakraborty et al. (2018).

FTIR data of the current study show the percentage of transmission spectra to identify any potential chemical reaction that might have occurred between the silymarin and the polymer nanoparticle (chitosan). The defined functional groups agree with More et al. (2019), who showed that the frequencies can serve as

a probe for identifying surface functional groups and their interactions. Due to different functional groups, the FT-IR spectra showed characteristic bands. The FT-IR spectrum of S-CsNPs showed an absorption band at 3757.33 and 3433.29 cm^{-1} (O–H stretching, Phenols/Alcohols), and this result agreed with the findings of Sharma et al. (2018), 2924.09 and 2856.58 cm^{-1} (C–H stretching, Alkanes) agreed with findings of Alshehri et al. (2022), 1730.15 cm^{-1} (C=O stretching, Esters), 1637.56 (C=O stretching carbonyl group), 1454.33 and 1390.68 cm^{-1} (C-H alkanes group), and 1136.07 cm^{-1} (related to the stretching vibrations of carbon-oxygen bonds (C-O alcohol)) were agreed with the report of Yousaf et al. (2019). Based on the results, the presence of hydroxyl and amine groups in chitosan and hydroxyl and carbonyl groups in S-CsNPs, indicates chemical interaction between the two compounds. Also, changes in the functional groups indicate they are related to forming new compounds. These results agreed with the findings of Agarwal et al. (2018), Almukhtar and Karam (2020), and Sherikar et al. (2021), who exhibited that the shifted peaks refer to the formation of a new compound.

The results of SEM indicated that the S-CsNPs are disseminated as separate NPs with clear-cut spherical shapes and homogeneously dispersed with a diameter range of 25.81-43.03 nm, which is in agreement with the findings of Sharma et al. (2018) and Sher et al. (2023). Atomic Force In AFM, the highest frequencies of particle sizes ranged from 40 to 50 nm, with sizes extending from 0 to 80 nm. The mean height was 11.40 nm, indicating smooth and spherical particles distributed homogeneously, agreeing with the findings of Das et al. (2011).

XRD patterns of chitosan display the main peak at a 2θ value of 20.53° and an intensity level close to 1200 counts, and the peaks of S-CSNPs were 18.71◦, 22.68◦, 23.61◦, 25.62◦, 31.92◦, 33.98◦, 40.19◦, 42.30◦, 45.49◦, 46.24◦, 48.22◦, 52.51◦, 56.72◦, 58.14◦, 64.08◦ and 66.74 ◦. The presence of such characteristic peaks depicts a crystalline state, with its main peak at a 2θ value of 31.92°. This shift indicates a difference in the crystal structure between these two materials, with S-CSNPs being more crystalline than CS. The chitosan diffraction peak, initially observed at 20.53°, has shifted to a higher value of 31.92° in this study, likely due to the interaction of chitosan loaded with silymarin to form S-CSNPs. The XRD results suggest that particle size effects generally account for broadening peaks in crystalline XRD patterns. Broader peaks indicate smaller particle sizes and reflect the influence of experimental conditions on particle structures. Small crystals have limited reflection levels with low intensity, while large crystals have numerous levels with high intensity. Therefore, X-ray diffraction peaks are formed due to reflections from crystal levels, and a decrease in intensity is evident in the pattern of S-CSNPs, which exhibit suppressed peaks (Holder and Schaak, 2019). These findings are consistent with those of Anand et al. (2018), who reported that the pure chitosan diffraction peak, previously found at 20.20°, shifted to a lower value of 19.85°, likely due to the interaction of CS-NPs with TPP and the crystalline structure of CSNPs. Additionally, Kahdestani et al. (2021) found that variations among the patterns might be traced to changes in the molecular arrangement within the crystal lattice. The pattern of teicoplanin-loaded chitosan nanoparticles showed reduced peaks at 2θ values of 22° and 25°, indicating a decrease in intensity.

References

Agarwal M., Agarwal M.K., Shrivastav N., Pandey S., Das R., Gaur P. (2018). Preparation of chitosan nanoparticles and their in-vitro characterization. International Journal of Life-Sciences Scientific Research, 4(2): 1713-1720.

Almukhtar J.G.J., Karam F.F. (2020). Preparation characterization and application of Chitosan nanoparticles as drug carrier. Journal of Physics: Conference Series, 1664(1): 012071.

Alshehri F.S., Kotb E., Nawaz M., Al-Jameel S., Amin K.A. (2022). Preparation, characterization, and antibacterial competence of silymarin and its nano-formulation. Journal of Experimental Nanoscience, 17(1), 100-112.

Anand M., Sathyapriya P., Maruthupandy M., Hameedha

Beevi A. (2018). Synthesis of chitosan nanoparticles by TPP and their potential mosquito larvicidal application. Frontiers in Laboratory Medicine, 2(2): 72-78.

Atangana E., Chiweshe T.T., Roberts H. (2019). Modification of novel chitosan-starch cross-linked derivatives polymers: Synthesis and characterization. Journal of Polymers and the Environment, 27(5): 979-995.

Camini F.C., Costa D.C. (2020). Silymarin: Not just another antioxidant. Journal of Basic and Clinical Physiology and Pharmacology, 31(4): 20190206.

Chakraborty P., Mustafa V., Abraham J. (2018). Synthesis and characterization of chitosan nanoparticles and their application in removal of wastewater contaminants. Nature Environment and Pollution Technology, 17(2).

Das S., Roy P., Auddy R.G., Mukherjee A. (2011). Silymarin nanoparticle prevents paracetamol-induced hepatotoxicity. International Journal of Nanomedicine, 1291-1301.

Dimitrijevic R., Cvetkovic O., Miodragović Z., Simic M., Manojlović D., Jovic V. (2013). SEM/EDX and XRD characterization of silver nanocrystalline thin film prepared from organometallic solution precursor. Journal of Mining and Metallurgy, Section B: Metallurgy, 49(1): 91-95.

Du W.L., Xu Z.R., Han X.Y., Xu Y.L., Miao Z.G. (2008). Preparation, characterization and adsorption properties of chitosan nanoparticles for eosin Y as a model anionic dye. Journal of Hazardous Materials, 153(1-2): 152-156.

El-Ghaffar M.A.A., Hashem M.S. (2010). Chitosan and its amino acids condensation adducts as reactive natural polymer supports for cellulase immobilization. Carbohydrate Polymers, 81(3): 507-516.

Holder C.F., Schaak R.E. (2019). Tutorial on powder X-ray diffraction for characterizing nanoscale materials. Acs Nano, 13(7): 7359-7365.

Kahdestani S.A., Shahriari M.H., Abdouss M. (2021). Synthesis and characterization of chitosan nanoparticles containing teicoplanin using sol–gel. Polymer Bulletin, 78(2): 1133-1148.

Macit M., Duman G., Cumbul A., Sumer E., Macit C. (2023). Formulation development of Silybum marianum seed extracts and silymarin nanoparticles, and evaluation of hepatoprotective effect. Journal of Drug Delivery Science and Technology, 83: 104378.

More M.P., Chitalkar R.V., Bhadane M.S., Dhole S.D., Patil A.G., Patil P.O., Deshmukh P.K. (2019). Development of graphene-drug nanoparticle based supramolecular self assembled pH sensitive hydrogel as potential carrier for targeting MDR tuberculosis. Materials Technology, 34(6): 324-335.

Muzzarelli R.A. (2009). Chitins and chitosans for the repair of wounded skin, nerve, cartilage and bone. Carbohydrate Polymers, 76(2): 167-182.

Nasti A., Zaki N.M., De Leonardis P., Ungphaiboon S., Sansongsak P., Rimoli M.G., Tirelli N. (2009). Chitosan/TPP and chitosan/TPPhyaluronic acid nanoparticles: Systematic optimisation of the preparative process and preliminary biological evaluation. Pharmaceutical Research, 26(8): 1918-1930.

Oh J.W., Chun S.C., Chandrasekaran M. (2019). Preparation and in vitro characterization of chitosan nanoparticles and their broad-spectrum antifungal action compared to antibacterial activities against phytopathogens of tomato. Agronomy, 9(1). https://doi.org/10.3390/agronomy9010021

Pedroso-Santana S., Fleitas-Salazar N. (2020). Ionotropic gelation method in the synthesis of nanoparticles/microparticles for biomedical purposes. Polymer International, 69(5): 443-447.

Sarvamangala D.., Kondala K.., Murthy U.S.N.., Rao B.N., Sharma G.V.R., Satyanarayana R. (2013). Biogenic synthesis of AGNP's using *Pomelo* fruit – characterization and antimicrobial activity against Gram+ve and Gram-ve Bacteria. International Journal of Pharmaceutical Sciences Review and Research, 19(2): 30-35.

Sharma A., Puri V., Kakkar V., Singh I. (2018). Formulation and evaluation of silymarin-loaded chitosan-montmorilloite microbeads for the potential treatment of gastric ulcers. Journal of Functional Biomaterials, 9(3): 52.

Sher M., Hussain I., Khan F.A., Afridi H.H., Sher W.M., Gulfam N., Ahmad Z. (2023). Effect of silymarin particle size on its solubility and oral bioavailability, the enhancement of pharmacological actions. Journal of Population Therapeutics and Clinical Pharmacology, 30(18): 2527-2560.

Sherikar A., Siddique M.U.M., More M., Goyal S.N., Milivojevic M., Alkahtani S., Nayak A.K. (2021). Preparation and evaluation of silymarin-loaded solid eutectic for enhanced anti-inflammatory, hepatoprotective effect: in vitro–in vivo prospect.

Oxidative Medicine and Cellular Longevity, 2021: 1-13.

Voron'ko N.G., Derkach S.R., Kuchina Y.A., Sokolan N.I. (2016). The chitosan–gelatin (bio) polyelectrolyte complexes formation in an acidic medium. Carbohydrate Polymers, 138: 265-272.

Woo J.S., Kim T.S., Park J.H., Chi S.C. (2007). Formulation and biopharmaceutical evaluation of silymarin using SMEDDS. Archives of Pharmacal Research, 30: 82-89.

Yousaf A.M., Malik U.R., Shahzad Y., Mahmood T., Hussain T. (2019). Silymarin-laden PVP-PEG polymeric composite for enhanced aqueous solubility and dissolution rate: Preparation and in vitro characterization. Journal of Pharmaceutical Analysis, 9(1): 34-39.